

Developing a Hybrid Data-Driven, Mechanistic Virtual Flow Meter - a Case Study

M. Hotvedt* B. Grimstad** L. Imsland*

* *Engineering Cybernetics Department, NTNU, Trondheim, Norway*
(e-mail: {mathilde.hotvedt, lars.imsland}@ntnu.no)

** *Solution Seeker (e-mail: bjarne.grimstad@solutionseeker.no)*

Abstract: Virtual flow meters, mathematical models predicting production flow rates in petroleum assets, are useful aids in production monitoring and optimization. Mechanistic models based on first-principles are most common, however, data-driven models exploiting patterns in measurements are gaining popularity. This research investigates a hybrid modeling approach, utilizing techniques from both the aforementioned areas of expertise, to model a well production choke. The choke is represented with a simplified set of first-principle equations and a neural network to estimate the valve flow coefficient. Historical production data from the petroleum platform *Edvard Grieg* is used for model validation. Additionally, a mechanistic and a data-driven model are constructed for comparison of performance. A practical framework for development of models with varying degree of hybridity and stochastic optimization of its parameters is established. Results of the hybrid model performance are promising albeit with considerable room for improvements.

Keywords: hybrid modeling, virtual flow metering, petroleum production systems

1. INTRODUCTION

For a petroleum asset to succeed economically, the operators have to, on a daily basis, make crucial decisions regarding optimization of the asset. Knowledge regarding the multiphase flow rates in the asset is therefore of high importance. The flow rates may be obtained through for example deduction well testing, test separators and multiphase flow meters (MPFM), however, these methods are costly and MPFMs call for well intervention upon failure (Marshall and Thomas, 2015). An alternative is virtual flow meters (VFM) that take advantage of measurements to describe the input-output relationship of a system with a mathematical model (Toskey, 2012).

There are several types of VFM models. Dependent on the amount of available process data and prior knowledge of the system, the types may be placed on a scale ranging from mechanistic models (M-models) derived from first-principles, to data-driven models (DD-models), which are generic mathematical models fitted to input-output data (Stosch et al., 2013), see Fig. 1. Often, the two extremes are called white-box and black-box models, with reference to the extent of prior knowledge about the system, for instance relationship between variables and physical interpretation of the parameters. The models in between are hybrid models (H-models) or grey-box models, which utilize modeling techniques from both fields and have a mixture of physical and non-physical parameters.

In this research, an H-model of a well production choke is developed using historical production data from the petroleum platform *Edvard Grieg* (Lundin Norway, 2019). In addition, an M-model and a DD-model are developed

for comparison of performance. A practical framework facilitating development of models with varying degree of hybridity and stochastic optimization of model parameters is constructed and conveniently enables future research into the field of hybrid modeling. Background into VFM modeling and the contributions of this research is given in Section 2, the three model types of the production choke is presented in Section 3, the practical framework is outlined in Section 4, the *Edvard Grieg* case study is presented in Section 5, before simulation results and a conclusion is given in Sections 6 and 7.

2. BACKGROUND

2.1 Virtual flow meter modeling approaches

The most common way to model VFM in today's oil and gas industry are with M-models, where some well known commercial VFM are Olga, K-Spice and FlowManager (Bikmukhametov and Jäschke, 2019). A great advantage with M-models is their way of representing prior knowledge through the use of first-principles, which leads to interpretable parameters and usually good extrapolation abilities. However, in order for M-models to be computationally feasible, model simplifications are usually a necessity and plant-model mismatch is unavoidable (Solle et al., 2016). Additionally, in complex processes, unknown physical relations are oftentimes present and difficult to capture. VFM with DD-models have shown promising performance suitable for real-time monitoring, without the need of prior knowledge about the system (AL-Qutami et al., 2018). Further, unknown phenomena may be captured if reflected in the process measurements. However,

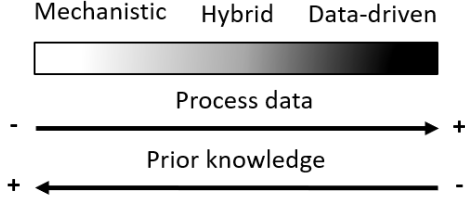


Fig. 1. Range of VFM models from mechanistic to data-driven, white-box to black-box.

DD-models are data hungry (Fig. 1), they struggle with extrapolation in unseen operational settings, parameters generally lack physical interpretation and incorporating process constraints is challenging. Several industrial and academic M- and DD-models are reported in Balaji et al. (2018); AL-Qutami et al. (2018); Bismukhametov and Jäschke (2019).

An in-between solution designed to utilize the best of both worlds are H-models, a concept widely used in literature. For instance, most M-models could be considered hybrid as real data is typically used for parameter estimation and model validation. Further, a DD-model trained on generated data from an M-model could also be regarded as hybrid (Solle et al., 2016), yet on the far right of the scale in Fig. 1. Similarly, methods utilizing measurements for online updates of the model or parameters, such as the Kalman Filter, could be considered hybrid. However, the end result of the model, used in monitoring or optimization, is either a fully M- or a fully DD-model. In this article, H-models are defined as follows

Definition A hybrid model consists of first-principle equations and generic mathematical structures.

Expectantly, compared to an M-model, the H-model should have an increased ability to capture unknown phenomena, yet have better interpretability than a fully DD-model through the inclusion of prior knowledge and physical parameters. Generally, the DD-part in the H-model will be smaller (in terms of number of parameters) than a fully DD-model and should thus require fewer data samples to obtain a satisfactory approximation of the process (Psychogios and Ungar, 1992), see Fig. 1.

A combination of an M- and a DD-model into an H-model may be done in two ways fundamentally, serial or parallel, illustrated in Fig. 2. Examples of serial models are parameter estimation with a DD-model (1a), a DD-model to capture unknown physical phenomena or modeling errors (1b) and equations utilized to construct specialized features as input to the DD-model, called feature engineering (1b). A parallel H-model (type 2) would be achieved if a composition of M- and DD-submodels are connected or used in an ensemble model. Naturally, combinations of the two fundamental ways will also be an H-model.

2.2 Hybrid models in literature

Some of the earliest reported H-models are within the field of chemistry. For instance, Psychogios and Ungar (1992) used a neural network for parameter estimation in a fedbatch bioreactor. On the other hand, H-models for

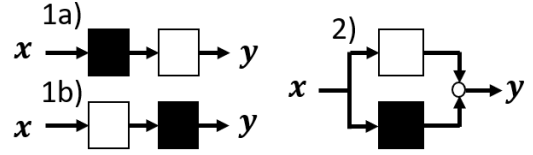


Fig. 2. Illustration of hybrid model variants. Serial H-models (type 1) and parallel H-models (type 2).

VFM are rare although some examples exist in literature. For instance, Xu et al. (2011) used feature engineering in a neural network for wet gas metering. Although feature engineering has shown to boost DD-models, choosing appropriate features is challenging (Sutton and Barto, 2018). Al-Rawahi et al. (2012) used a neural network algorithm to estimate the mixture density of multiphase flow. However, the neural network required measurements from a MPFM, such as capacitance, which may not be as readily available as other measurements. Additionally, MPFM are known to require frequent calibration and may yield high measurement error in-between calibrations (Falcon et al., 2001). Although not a VFM, Baraldi et al. (2014) used an H-ensemble model to detect degradation of production choke valves.

2.3 Contributions

The contributions of this research are two-fold:

- A hybrid VFM model for production chokes is developed and validated utilizing real historical production data with readily available measurements such as pressures, temperatures and choke openings.
- A practical and convenient framework to facilitate development of models with varying degree of hybridity and stochastic optimization of the model parameters.

It must be specified that the main goal of this research has not been to find an H-model that outperforms its M- and DD-model equivalent, but to illustrate that an H-model may offer advantages over M- and DD-models. Additionally, an ambition has been to establish a convenient framework for future research into hybrid modeling. In that manner, only one type of H-model has been developed, type 1a, with parameter estimation using a neural network in an M-model. However, in this case, the developed framework facilitate training of the model without requiring measurements of the parameter to be estimated. This will be explained in Section 4.

3. CHOKE MODELS

A production choke may be illustrated as in Fig. 3, where the volumetric oil flow rate, Q_o , will be estimated using nearby measurements such as pressures (p), temperatures (T) and choke opening (z). The three model types of the production choke (M, H, DD) are described in the following sections. For all models, data sets containing measurements of Q_o are required to optimize the model, that is, to find or learn the parameters that minimize the deviation between the measured (Q_o^m) and estimated (Q_o^e) oil flow rate.

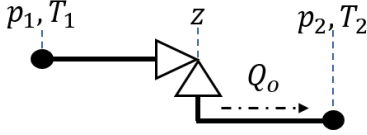


Fig. 3. Illustration of the well production choke

3.1 Mechanistic model

The M-model is taken from Kittelsen et al. (2014) and described with the equations (1)-(7).

$$Q_o = \frac{x_o w}{\rho_o, ST} \left[\frac{Sm^3}{h} \right] \quad (1)$$

$$w = NC_v(z) \sqrt{Y^2 \rho_c (p_1 - p_2)} \left[\frac{kg}{h} \right] \quad (2)$$

$$Y^2 = \left(1 - \frac{1}{3} \frac{x_{lim}}{x_{TP}}\right)^2 \frac{x_{lim} p_1}{p_1 - p_2} \quad [-] \quad (3)$$

$$\frac{1}{\rho_c} = \frac{x_g}{\rho_g} + \frac{x_l}{\rho_l} + \frac{1 - x_o - x_g}{\rho_w} \left[\frac{m^3}{kg} \right] \quad (4)$$

$$\rho_g = \frac{M_w p_1}{z_g R T_1} \left[\frac{kg}{m^3} \right] \quad (5)$$

$$x_{lim} = \min(x_P, x_{TP}) \quad [-] \quad (6)$$

$$x_P = \frac{p_1 - p_2}{p_1}, x_{TP} = \frac{p_1 - p_2}{p_1} \Big|_{critical} \quad (7)$$

N is a conversion factor, z_g is the gas compressibility factor calculated with a correlation from Sutton (1985), the liquid densities, ρ_o and ρ_w , are assumed constant (ST for standard conditions), and the $C_v(z)$ is the valve flow coefficient determined with linear interpolation between a given set of test points. The test points are usually from lab-experiments with water, yet calibrated to the multiphase flow once in place. The fluid mass fractions, x_i for $i \in \{o, g, w\}$, are often estimated from well-tests, for instance using measurements from a test-separator, and updates are generally infrequent. The metric x_{TP} represents critical flow through the choke and occur at $\frac{p_2}{p_1} \approx 0.6$ (Jansen, 2015), yielding $x_{TP} \approx 0.4$. Further nomenclature may be found in Kittelsen et al. (2014). In this research, ρ_o , ρ_w , and a multiplicative constant for the $C_v(z)$; $a \cdot C_v(z)$, are chosen as learnable parameters. The multiplicative constant is chosen for simplicity although individual test points may be adjusted if desired. The parameter vector is thus $\theta_m = [\rho_o, \rho_w, a]$. As the parameters are physical, regularization is employed to keep them within feasible bounds. However, in an attempt at introducing some flexibility in the model, the a is not regularized. The optimization and regularization of the parameters will be further explained in Section 4.

3.2 Data-driven model

The DD-model is a fully-connected, feed forward neural network with seven inputs $\{p_1, p_2, T_1, T_2, z, x_o, x_g\}$, and one output $\{Q_o\}$. The learnable parameters are the weights and biases on each layer, $\theta_{dd} = [\mathbf{W}_{dd}, \mathbf{b}_{dd}]$. The neural network architecture (width/depth) is chosen in the tuning process and will be described in Section 5. The Rectified Linear Unit (ReLU) is used as activation function and ℓ_2 -regularization is employed to avoid overfitting the network.

3.3 Hybrid model

The H-model (type 1a, Fig. 2) is represented with the equations in (1)-(7), but with the C_v obtained from a fully-connected, feed forward, neural network with inputs $\{z, x_o, x_g\}$ and ReLU as activation function. The mass fractions were included as inputs due to an analysis of the data set that indicated a correlation between the C_v and the mass fractions. Due to page limitations, the analysis is not included. The learnable parameters are the liquid densities and the weights and biases of the neural network, $\theta_h = [\rho_o, \rho_w, \mathbf{W}_h, \mathbf{b}_h]$. The neural network architecture is chosen in the tuning process and parameter regularization is employed to keep the physical parameters within specified bounds and to prevent overfitting of the neural network, see Section 4.

4. MODELING FRAMEWORK

To easily investigate different model types, a practical framework utilizing machine learning techniques is constructed¹. The framework enables a smooth transition between implementing and optimizing a fully M-model to a fully DD-model. It consist of several parts and will be defined in the following.

4.1 Defining the model

This part enables a convenient way to implement models with varying degree of hybridity. Firstly, the model parameters must be defined, either as single, learnable parameters, as for the physical parameters, or as neural networks with weights and biases. Effortlessly, a model will move on the scale from an M-model to a DD-model (Fig. 1) dependent on the defined parameters. Thereafter, the forward pass of the input data \mathbf{x} must be implemented as a function of the model parameters, $\hat{\mathbf{y}} = f(\mathbf{x}; \theta)$. The forward pass is defined as a computational graph, enabling access to the model derivatives through automatic differentiation. In this case study, the forward pass for the M-model is the mechanistic equations in (1)-(7), $\hat{\mathbf{y}}_m = f_m(\mathbf{x}_m; \theta_m)$. For the H-model, some of the inputs, \mathbf{x}'_h , is firstly propagated through a neural network to estimate the C_v , $C_v = f_{cv}(\mathbf{x}'_h; \mathbf{W}_h, \mathbf{b}_h)$, which is thereafter used in equation (2). This composition is defined as $\hat{\mathbf{y}}_h = f_h(\mathbf{x}_h; \theta_h)$. A particularly appealing property with this H-model type is that measurements of the C_v are not required as the model is trained on the output Q_o . Lastly, the forward pass for the DD-model is simply propagation of the input data through the neural network, $\hat{\mathbf{y}}_{dd} = f_{dd}(\mathbf{x}_{dd}; \theta_{dd})$.

4.2 Defining the optimization problem

Once the model is defined, a general optimization problem to find the parameters that minimizes the deviation between the model estimates $\hat{\mathbf{y}} = \mathbf{Q}_{o, \xi}^e = f_{\xi}(\mathbf{x}_{\xi}; \theta_{\xi})$ where $\xi \in \{m, h, dd\}$ and the measurements $\mathbf{y} = \mathbf{Q}_o^m$ may be set up as

¹ We have utilized PyTorch, but other possibilities exist such as TensorFlow.

$$\begin{aligned}\hat{\theta}_\xi &= \arg \min_{\theta_\xi} J(\theta_\xi, \lambda_\xi) \\ &= \arg \min_{\theta_\xi} \left(\frac{1}{n} \sum_{i=1}^n \left(y^{(i)} - f_\xi(\mathbf{x}_\xi^{(i)}; \theta_\xi) \right)^2 \right. \\ &\quad \left. + \frac{1}{n} \sum_{j=1}^p \lambda_{j,\xi} (\theta_{j,\xi} - \mu_{j,\xi})^2 \right)\end{aligned}\quad (8)$$

The first term in eq. (8) is the mean square error (MSE) and the second is an ℓ_2 -regularization term with regularization factors λ_i . For the physical parameters in the M- and H-model, the goal of regularization is to penalize deviation of the parameters from a prior (expected) value, μ_i . For the neural network parameters, common practice is followed and μ_i is set to zero. For the physical parameters, maximum a posteriori (MAP) estimation has been set up to automatically calculate the λ_i factors, see Section 4.3. If measurements of the output are available from different sources, additional MSE terms may be added and weighted according to the uncertainty in the measurement source. In this research, only measurements from a MPFM has been utilized.

The framework solves the optimization problem in eq. (8) using iterative gradient-based optimization. The update formula may be stated as follows

$$\theta_\xi^{k+1} = \theta_\xi^k - \alpha^k \mathcal{M}(\mathbf{x}_\xi^{k'}; \theta_\xi^k, \lambda_\xi) \quad (9)$$

where α^k is the learning rate (or step-size), $\mathbf{x}_\xi^{k'}$ is a subset of the data samples and \mathcal{M} is the set of equations calculating the step direction. Different algorithms may be selected, such as stochastic gradient descent (SGD), AdaDelta, AdaGrad, Adam among others (Bottou et al., 2018). Stochastic gradient-based optimization algorithms has the advantage of being well suited for large scale models, either in terms of large data-sets or many parameters (Bengio, 2012). For instance SGD, $\mathcal{M} = \nabla_{\theta} \tilde{J}(\mathbf{x}; \theta^k, \lambda)$, where $\nabla \tilde{J}$ may be calculated using only one sample (SGD), a subset of samples (mini-batch SGD) or all samples (batch SGD). Knowing which optimization algorithm yields the best result is challenging as it might be problem dependent. Therefore, the framework promote investigation of different optimization algorithms. In this research, Adam with mini-batches is used for all models.

4.3 Calculation of regularization parameters

The λ_i regularization factors for the physical parameters may be automatically calculated through MAP estimation. If one assumes a model of the form

$$y = f(x; \theta) + \epsilon \quad \epsilon \sim \mathcal{N}(0, \sigma_\epsilon^2) \quad (10)$$

the MAP estimation may be set up as follows utilizing Bayes' rule, where (X, y) is the collection of data points

$$\hat{\theta}_{MAP} = \arg \max_{\theta} (\log p(y|X, \theta) + \log p(\theta)) \quad (11)$$

If one additionally assumes independent Gaussian priors of the parameters $\theta_i \sim \mathcal{N}(\mu_i, \sigma_i^2)$, the MAP estimation will result in, after some rearrangements,

$$\begin{aligned}\hat{\theta}_{MAP} &= \arg \min_{\theta} \left(\sum_{i=1}^n \left(y^{(i)} - f(x^{(i)}; \theta) \right)^2 \right. \\ &\quad \left. + \sum_{i=1}^p \frac{\sigma_\epsilon^2}{\sigma_i^2} (\theta_i - \mu_i)^2 \right)\end{aligned}\quad (12)$$

Dividing by n and setting $\lambda_i = \frac{\sigma_\epsilon^2}{\sigma_i^2}$, the MAP estimation will be the same as the estimate in eq. (8). The σ_i may be determined based on physical bounds and if σ_ϵ is known, λ_i is automatically calculated. In practice, σ_ϵ must be tuned, however, the number of coefficients to determine decreases with this approach.

5. CASE STUDY - EDVARD GRIEG

To develop the three model types defined in Section 3 and analyze and compare the performance, historical production data from *Edvard Grieg* has been utilized. In addition to pressures, temperatures, and choke opening (see Fig. 3), measurements from a MPFM located upstream the choke restriction was used for training the model, keeping in mind that MPFM measurements may be faulty and require frequent calibration (Falcon et al., 2001). Future work should include well-tests which in general have higher accuracy than MPFM measurements. The production data are from 10 oil wells, yielding a total of 30 models, over a period of 1248 days. Consequently, the assumption of constant parameters, for instance the liquid densities and the C_v -curve, may be a rough approximation and future work should consider updating the models at certain intervals in time to account for changes in the true process.

The data was preprocessed in two steps before performing modeling. First, the raw production data was processed by Solution Seeker's data squashing technology (Grimstad et al., 2016). The data squashing algorithm partitions the data into intervals of steady-state operation. The data in each interval is then compressed to mean values using statistics suitable for time-series data. The result is a compressed data set of steady-state operating points, suitable for steady-state modeling. In the second preprocessing step, samples considered invalid, such as samples with unrealistically large well head pressures or negative flow rates, were removed and some samples were slightly modified, for instance small negative flow rates, where measurement noise was the likely cause of error. The second step resulted in a variable number of samples per well, in the range 612-2175. Further, for all models, the mass fractions were calculated using MPFM flow rates and standard densities. In an industrial setting, the mass fractions are often calculated from sparse well-test samples, thus to mimic this setting, a mass fraction update time of 30 days was employed, using an average of the last 20 samples.

The data set of each well was divided into two, training (75%) and test (25%), where 15% of the latest training data was used as a validation set to decide upon the hyperparameters. An ambition was for the three model types to generalize well across all wells of the asset. Consequently, the same set of hyperparameters was used for a model type, instead of individual tuning of each model type for each well. However, one should expect a lower overall error by individual tuning due to dissimilar well operating conditions and variable sample numbers, and this should be considered in future work. The average root mean square error (RMSE) and average mean absolute error (MAE) of the 10 wells were monitored and the best set of hyperparameters was chosen based on the minimum obtained averages. However, if prominent overfitting oc-

curred in a well for a set of hyperparameters, that is, if the validation error increased when the training error decreased towards the end of training, the next best set of hyperparameters was chosen. Practical recommendations from Bengio (2012) was followed in the tuning process.

For all models, the learning rate (α) was thoroughly experimented with as this often is the most important hyperparameter to tune (Bengio, 2012). Further, for the M-model, the physical parameters had to converge within the specified bounds, thus, the number of epochs (E), that is, the number of loops through the training set, and σ_ϵ were tuned thereafter. For the H-model, in addition to convergence of the physical parameters, training of the neural network had to be taken into account. However, E may be high and the neural network architecture (width/depth) large without leading to overfitting of the neural network as long as regularization of the neural network parameters is applied (Bengio, 2012). Hence, E was set sufficiently high and σ_ϵ adjusted for convergence of the physical parameters within bounds, the width/depth was set to 20/2 and combinations of α and the neural network regularization factor, $\lambda_{i,nn}$, were tested. For the DD-model, the same recommendations were followed. The E was set high and combinations of α and $\lambda_{i,nn}$ investigated. The width/depth was set to 70/2. Lastly, the batch size (B) is often tuned independently of the other hyperparameters (Bengio, 2012) and was thus tuned last.

An overview of the final hyperparameters are given in Table 1. Observe that the M-model required a larger σ_ϵ than the H-model for the physical parameters to converge within specified bounds, indicating that the H-model accounts for some of the measurements noise with the DD-part. Further, the best performance for the H-model was obtained with a low batch number, however, only small differences in average error lead to this choice.

Table 1. Overview of the final model hyperparameters

	M-model	H-model	DD-model
E	5000	2000	2000
B	150	32	150
α	0.01	0.01	0.01
σ_ϵ	25	10	-
$\lambda_{i,nn}$	-	0.01	0.001
width/depth	-	20/2	70/2

6. SIMULATION RESULTS

The simulation results are shown in Fig. 4, where the RMSE and MAE of the test set for the 10 wells are illustrated, and Fig. 5 which is a cumulative deviation plot (CDP) (Corneliussen et al., 2005) indicating the accuracy of the developed VFM models, that is, how many of the test points fall within a certain deviation from the measurement.

There are several interesting observations to be made from the results. Firstly, notice the extreme outlier that is present in the DD-model performance in Fig. 4. The outlier is caused by one of the wells for which all the models yielded a high error. An analysis of the test set for this well indicate an operational setting very different from the setting in the training set. As mentioned in

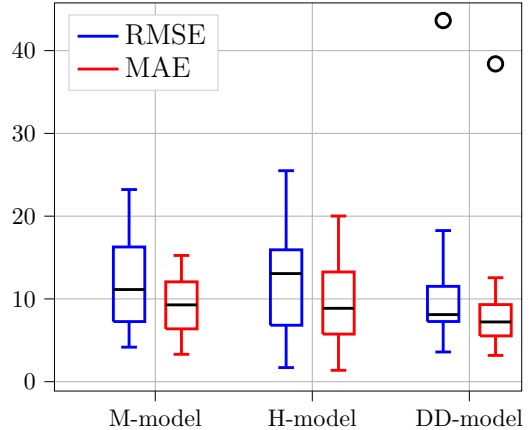


Fig. 4. Boxplot overview with median for the three model types across the 10 wells.

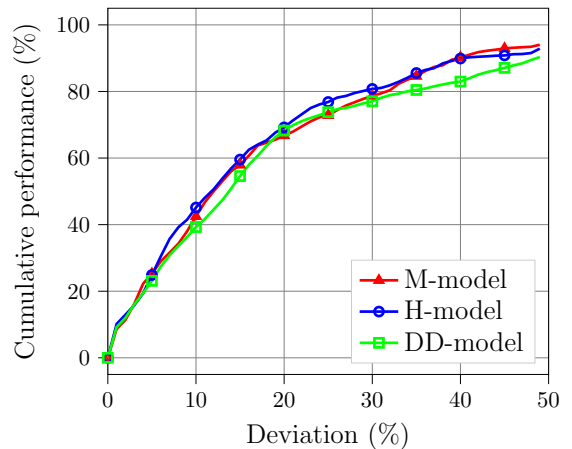


Fig. 5. Cumulative deviation plot of all test samples across the 10 wells.

Section 2, DD-models may struggle with extrapolation in unseen operational settings which may explain the outlier. In that case, the results also indicate that the H-model has preserved some of the extrapolation power of the M-model which do not have the extreme outlier. Another interesting observation in Fig. 4, even though the DD-model has the shortest distance between the quartiles and the lowest median errors, the H-model has the lowest error on some of the wells. This may indicate the H-models ability to leverage the DD-part to capture unknown phenomena yet still provide high physical interpretation through the M-part. Naturally, these results are only preliminary and further investigations are necessary.

Generally, the results show a higher error than expected. Other studies have reported almost 90% performance for 20% deviation in the CDP (e.g. AL-Qutami et al. (2018)), whereas in this paper about 70% performance for 20% deviation is achieved. There may be several causes for the large error. Firstly, preprocessing of the data could be improved by for instance further outlier removals. In addition, MFPM measurements was used for mass fraction calculation and in training despite, as previously stated, a possibility of being faulty in between calibrations. Further, the mass fractions was updated every 30 days to mimic an industrial setting, however, in training, continuous

mass fraction updates could be utilized. Hence, future work should include measurement sources with higher accuracy, such as well-tests, and analyze performance with continuous mass fraction updates. Secondly, the model types were generalized across all wells and improved results would most likely be achieved with individual tuning. As an example, for one of the wells more than 90% performance was achieved at 20% deviation. Further, utilization of a more accurate mechanistic choke model or optimization of additional physical parameters may decrease the error in the M- and H-model. Thirdly, the number of days for which the models are used in prediction should be taken into account. For some of the wells, the test set covered more than 200 days, whereupon the true process could have changed significantly and the models lack validity. Future work should consider online training of the models at regular intervals in time. Nonetheless, the main goal of this research, stated in Section 2.3, was not to find exceptional models, but to illustrate that an H-model may offer advantages over M- and DD-models and to establish a framework for convenient future research.

7. CONCLUSION

Results in Section 6 indicate that hybrid modeling is promising and may offer advantages over both mechanistic and data-driven modeling. However, results are preliminary and there is considerable room for improvements. Future work should put more effort into preprocessing of the data set, analysis of the mass fraction calculation influence on performance and inclusion of well tests in training and validation. Further, individual tuning of each well should be investigated and the models should be tested with different data sets, for instance from other petroleum assets. Last but not least, future work should explore different hybrid model variants, for which the presented framework is convenient and highly suitable.

ACKNOWLEDGEMENTS

This research is a part of BRU21 - NTNU Research and Innovation Program on Digital and Automation Solutions for the Oil and Gas Industry (www.ntnu.edu/bru21) and supported by Lundin Norway AS.

REFERENCES

- AL-Qutami, T., Ibrahim, R., Ismail, I., and Ishak, M.A. (2018). Virtual multiphase flow metering using diverse neural network ensemble and adaptive simulated annealing. *Expert Systems With Applications*, 93, 72–85.
- Al-Rawahi, N., Meribout, M., Al-Naamany, A., Al-Bimani, A., and Meribout, A. (2012). A neural network algorithm for density measurement of multiphase flow. *Multiphase Science and Technology*, 24, 89–103.
- Balaji, K., Rabiei, M., Suicmez, V., Canbaz, C., Agharzeyva, Z., Tek, S., Bulut, U., and Temizel, C. (2018). Status of data-driven methods and their application in oil and gas industry. *Society of Petroleum Engineers*.
- Baraldi, P., Mangili, F., Gola, G., Nystad, B., and Zio, E. (2014). A hybrid ensemble-based approach for process parameter estimation and degradation assesment in offshore oil platforms. *International Journal of Perfromability Engineering*, 10, 497–509.
- Bengio, Y. (2012). *Practical Recommendations for Gradient-Based Training of Deep Architectures*. In: *Montavon G., Orr G.B., Mller KR. (eds) Neural Networks: Tricks of the Trade. Lecture Notes in Computer Science.*, volume 7700, 437–478. Springer, Berlin, Heidelberg.
- Bikmukhametov, T. and Jäschke, J. (2019). First principles and machine learning virtual flow metering: a literature review. *Journal of Petroleum Science and Engineering*, 4, 3037–3043.
- Bottou, L., Curtis, F., and Nocedal, J. (2018). Optimization methods for large-scale machine learning. *Society for Industrial and Applied Mathematics*.
- Corneliusson, S., Couput, J.P., Dahl, E., Dykesteen, E., Frøysa, K.E., and Malde, E. (2005). Handbook of multiphase flow metering. *Norwegian Society for Oil and Gas Measurement (NFOGM)*, 2. revision.
- Falcon, G., Hewitt, G., Alimonti, C., and Harrison, B. (2001). Multiphase flow metering: current trends and future developments. *SPE Annual Technical Conference and Exhibition*.
- Grimstad, B., Gunnerud, V., Sandnes, A., Shamlou, S., Skrondal, I.S., Uglane, V., Ursin-Holm, S., and Foss, B. (2016). A Simple Data-Driven Approach to Production Estimation and Optimization. In *SPE Intelligent Energy International Conference and Exhibition*. Society of Petroleum Engineers.
- Jansen, J.D. (2015). *Nodal Analysis of Oil and Gas Well*. Delft University of Technology.
- Kittelsen, P., Fjalestad, K., and Aasheim, R. (2014). Stabilized and increased well production using automatic choke control. *Society of Petroleum Engineers*.
- Lundin Norway (2019). Norway - edvard grieg. <https://www.lundin-petroleum.com>.
- Marshall, C. and Thomas, A. (2015). Maximising economic recovery - a review of well test procedures in the north sea. *Society of Petroleum Engineers*.
- Psychogios, D. and Ungar, L. (1992). A hybrid neural network-first principles approach to process modeling. *AIChE Journal*, 30, 1499–1511.
- Solle, D., Hitzmann, B., Herwig, C., Remelhe, P.M., Ulonska, S., Wuerth, L., Prata, A., and Steckenreiter, T. (2016). Between the poles of data-driven and mechanistic modeling for process operation. *Chemie Ingenieur Technik*.
- Stosch, M., Oliveria, R., Peres, J., and Azevedo, S. (2013). Hybrid semi-parametric modeling in process system engineering: Past, present and future. *Computers and Chemical Engineering*.
- Sutton, R. (1985). Compressibility factors for high-molecular-weight reservoir gases. *SPE Annual Technical Conference and Exhibition*.
- Sutton, R. and Barto, A. (2018). *Reinforcement Learning, an introduction*. The MIT Press, Cambridge, Massachusetts, London, England.
- Toskey, E. (2012). Improvements to deepwater subsea measurements rpsea program: Evaluation of flow modeling. *Offshore Technology Conference*.
- Xu, L., Zhou, W., Li, X., and Tang, S. (2011). Wet gas metering using a revised venturi meter and soft-computing approximation techniques. *IEE transactions on instrumentation and measurement*, 60, 947–956.